

A Comparative Analysis of Influenza Vaccination Programs

Shweta Bansal ¹, Babak Pourbohloul ², Lauren Ancel Meyers ^{3,4}

1. Computational and Applied Mathematics, University of Texas at Austin.
2. University of British Columbia Centre for Disease Control; and Health Care and Epidemiology, Faculty of Medicine, University of British Columbia
3. Section of Integrative Biology and Institute for Cellular and Molecular Biology, University of Texas at Austin.
4. Santa Fe Institute, External Faculty, Santa Fe, New Mexico

Corresponding Author: laurenmeyers@mail.utexas.edu

SUMMARY

Background

The threat of avian influenza and the 2004-2005 influenza vaccine supply shortage in the United States has sparked a debate about optimal vaccination strategies to reduce the burden of morbidity and mortality caused by the influenza virus.

Methods and Findings

We present a comparative analysis of two classes of suggested vaccination strategies: mortality-based strategies that target high risk populations and morbidity-based that target high prevalence populations. Applying the methods of contact network epidemiology to a model of disease transmission in a large urban population, we evaluate the efficacy of these strategies across a wide range of viral transmission rates and for two different age-specific mortality distributions.

We find that the optimal strategy depends critically on the viral transmission level (reproductive rate) of the virus: morbidity-based strategies outperform mortality-based strategies for moderately transmissible strains, while the reverse is true for highly transmissible strains. These results hold for a range of mortality rates reported for prior influenza epidemics and pandemics. Furthermore, we show that vaccination delays and multiple introductions of disease into the community have a more detrimental impact on morbidity-based strategies than mortality-based strategies.

Conclusion

If public health officials have reasonable estimates of the viral transmission rate and the frequency of new introductions into the community prior to an outbreak, then these methods can guide the design of optimal vaccination priorities. When such information is unreliable or not available, as is often the case, this study recommends mortality-based vaccination priorities.

INTRODUCTION

In response to the 2004-2005 influenza vaccine shortage, the United States Centers for Disease Control and Prevention (CDC) restricted vaccines to those most at risk for hospitalization and death — healthy infants, elderly, and individuals with chronic illnesses. This strategy may be limited by the failure of vaccines to yield adequate protection for high-risk individuals [1,2] and the lesser roles played by infants and elderly in disease transmission— they typically do not introduce influenza into households or other social groups.

Influenza outbreaks are believed to hinge, instead, on transmission by healthy school children [3-6], college students, and employed adults who have many daily contacts and are highly mobile [7]. Thus epidemiologists have suggested an alternative approach: vaccinate school-age children to slow the spread of disease and thereby indirectly decrease mortality [8,9]. Several studies support this strategy. Monto et al. immunized school children in Tecumseh, Michigan with inactivated influenza vaccine in 1968 and found lower total morbidity than that in a matching community during a wave of influenza A (H3N2) [10]. Reichart et al. argue that mandatory influenza vaccination of school children in Japan from 1962 to 1987 reduced incidence and mortality among the elderly [11]. Recently, Longini et al. used mathematical models to show that, under certain assumptions, vaccinating 80% of all school-age children is almost as effective as vaccinating 80% of the entire population [8]. School-based vaccination programs have the additional benefits of high coverage, high efficacy and minimal side effects [12].

In a similar spirit, others have suggested contact-based priorities that target individuals with the highest numbers of potentially disease-causing contacts [13,14,35].

This assumes that vulnerability is directly proportional to the number of contacts, and that removing the most vulnerable individuals from the transmission chain will maximally decrease disease spread. Identifying high-contact individuals in a community, however, may be difficult in practice.

Here we apply tools from contact network epidemiology [15-17, 26] to evaluate vaccination strategies for a spectrum of influenza strains when vaccine supplies are limited. We use a realistic model of contact patterns in an urban setting to compare mortality-based strategies that target high-risk individuals to morbidity-based strategies that target demographics with high attack rates. We assess the efficacy of these measures for two substantially different virulence patterns, one based on mortality estimates from annual influenza epidemics and the other based on mortality estimates from the 1918 influenza pandemic. In both cases, under limited vaccine availability, morbidity-based strategies are preferred for moderately transmissible strains while mortality-based strategies are preferred for highly transmissible strains. Furthermore, both delays in vaccination and multiple imported cases decrease the relative effectiveness of morbidity-based strategies.

METHODS

Population Model

We built a *contact network model* that captures the interactions that underlie respiratory disease transmission within a city. The model is based on demographic information for Vancouver, British Columbia. In the model, each person is a *vertex* and interactions among people are *edges* between appropriate vertices. Each person is assigned an age

based on Vancouver census data, and age-appropriate activities (school, work, hospital, etc.). Interactions among individuals reflect household size, employment, school and hospital data for Vancouver. The model population includes ~257,000 individuals. For further details and sensitivity analysis, see Supporting Information.

Our contact network model contains *undirected* edges that reflect the possibility of disease transmission in either direction between two individuals, and *directed* edges that indicate the possibility of disease transmission from one person to another, but not the reverse. (See Figure 1.) Directed edges model the possibility of transmission from an infected member of the general public to health care workers (HCW) during hospital visits. In a typical epidemic, most individuals infected with influenza do not seek hospital care. We assume that only high-risk groups (infants and elderly) visit hospitals upon infection and thus have opportunities to infect the HCW's who treat them [18]. We also consider a more extreme scenario in which almost all infected individuals are at risk for serious complications and thus will seek medical care upon infection.

Influenza Mortality

Mortality rates differ both across demographic groups and among strains of influenza (see Table 3 and the Supporting Information), and thus the optimal vaccination priorities are likely to depend on the virulence of the circulating strains. We model two substantially different mortality models. The first assumes age-specific mortality rates typical of interpandemic outbreaks of flu, which are based on national viral surveillance data reported from 1977-1999 [21]. The rate is highest for elderly, followed by infants, who are most at risk for death caused directly by influenza or pneumonia or by primary

respiratory or circulatory complications. The second model, which was intentionally chosen for contrast, assumes mortality rates estimated for the 1918 flu pandemic. These are high for healthy young adults aged 20-40 and children under 5 and low for older children and the elderly [22] (Table 3). There are, however, conflicting estimates for the elderly [23,24]. We use a low estimate to achieve the greatest departure from the interpandemic model, and thus to ascertain the sensitivity of our results to assumptions about influenza mortality. Henceforth, we refer to these two models as *interpandemic* and *pandemic*, respectively. We consider other reported mortality rates in the Supporting Information.

Vaccine Priorities

We model targeted pre-season vaccination with single doses of inactivated influenza vaccine by removing select individuals (vertices) and all their contacts (edges) from the network before predicting the spread of influenza (see Figure 1). This assumes that each vaccinated individual is either fully protected or not protected at all (100% effectiveness). The fraction of the vaccinated population that becomes fully protected is based on demographic-specific vaccine efficacy estimates (Table 1). We evaluated four strategies (Figure 2): (1) a *mortality-based* strategy that, like the recent CDC strategy, targets demographics that are most vulnerable to health complications or death (infants, elderly, and health care workers for interpandemic flu; and infants, adults, and health-care workers for the case of pandemic flu); (2) a *morbidity-based* strategy, similar to the priorities suggested by Longini and Halloran [9] and Monto et al.[10], that targets school-aged children and school staff, and thereby aims to reduce mortality through herd

protection [19]; (3) a *mixed* strategy that targets demographics with high attack rates (children) and high mortality rates (infants and elderly for interpandemic flu; infants and adults for pandemic flu); and (4) a *contact-based* strategy that removes a fraction of the most connected individuals.

We modeled the mortality-based strategy by removing infants, elderly, and health care workers from the network based on reported maximum coverage and efficacy levels for these demographics [12,20] (Table 1). This yields 13% coverage of the total population (Table 2). We then implemented the remaining strategies to match this overall coverage level. Targeted groups are removed in proportion to demographic-specific vaccine coverage levels reported in the 2002 National Health Interview Survey by the CDC [20], and the vaccine efficacy levels based on age-specific rates reported for inactivated influenza vaccine [12].

Epidemiological Analysis

We define the transmissibility of a disease, T , as the average probability that an infectious individual will transmit the disease to a susceptible individual with whom they have contact. This summarizes important features of disease propagation including the contact rates among individuals, the duration of the infectious period, and the per contact probability of transmission. This per contact probability of transmission, in turn, summarizes the susceptibility (immune response) and the infectiousness (viral shedding) of individuals. Our analysis allows for variation in transmission rates from one individual to the next, but it assumes that these rates vary randomly with respect to the underlying contact patterns. There is evidence, however, that transmission rates may vary

systematically among demographics, and, in particular, may be highest for children [36]. In Supporting Information, we consider modified models that explicitly capture such demographic-specific variation in transmission rates and show that this additional complexity does not alter the results reported below.

T is linearly related to the key epidemiological parameter R_0 . In particular, R_0 is equal to $T \cdot \kappa$, where κ is a measure of the connectivity within the population (network) [25,26]. Intuitively, R_0 is largest for highly contagious pathogens (represented by a high T) spreading through densely connected populations (represented by a high κ). $R_0 = 1$ corresponds to a critical transmissibility value T_c , above which a population is vulnerable to large scale epidemics and below which only small outbreaks occur [25].

We use methods based on contact network epidemiology [15-17,25,26] to predict the fate of an influenza outbreak as a function of the average transmissibility T of the strain. For any contact network, one can mathematically predict the epidemic threshold (T_c), the average size of a small outbreak (s), the average size (S_e) and probability of a large-scale epidemic (P_e), and demographic-specific attack rates for an epidemic, should one occur. Mortality is predicted by multiplying the expected number of infections for a given group by the age-specific mortality rate assumed for that group. (See Supporting Information for additional details).

To verify these mathematical predictions, we perform numerical simulations of disease spread assuming a simple Susceptible-Infectious-Recovered (SIR) model. Beginning with a susceptible network and a single infected case, we iteratively take each currently infected vertex, infect each of its susceptible contacts with probability T and then change the status of the original vertex to “recovered.” These simulations are

generally consistent with the mathematical calculations (as demonstrated in Figure 4a), and thus we primarily report the analytical results.

Model Validation

We use data for the 1918 “Spanish Influenza” pandemic to perform a comparison of the attack rate predictions made by our model to those actually caused by the disease. Age-specific attack rate data for the 1918 pandemic was collected and reported by Wade Hampton Frost in 1920 [27]. The data is based on a survey of approximately 146,000 people (representing a cross-section of the U.S. population, which at the time numbered 103 million). Infection rates for influenza were based on self-reported responses by study participants.

There was no vaccination available for influenza at the time in the United States, so we use the population network described above with no implemented vaccination program. Using the methods described earlier, we perform epidemiological analysis and compute the attack rates predicted by our model for each demographic group. The results are shown in Figure 3. Given the reported age-specific attack rates, our model places the transmissibility of the virus for the 1918 pandemic at approximately $T = 0.09$ (or $R_0 = 1.8$). As a consistency check, this estimate agrees very closely to the recently revised estimate for the pandemic influenza reproductive rate [28], based on US and UK 1918 pandemic mortality data.

We made similar comparisons to data from the 1957 and 1968 pandemics, as well as interpandemic outbreaks during 1977-1980. There is, however, greater uncertainty around estimates for the reproductive numbers during these periods, which stems from

the specific data collection processes, relatively small sample sizes, and a lack of information about vaccine coverage and efficacy [3,5-7,10]. Due to this uncertainty, we are unable to report those comparisons here.

RESULTS & DISCUSSION

Direct vs. Indirect Intervention Methods

For interpandemic influenza, morbidity-based and contact-based strategies appear to offer significant indirect protection of non-vaccinated individuals who would otherwise become infected via transmission chains that have now been severed due to vaccination. Indeed, for all strains, these two strategies are predicted to yield the lowest attack rates (Figure 4a). If the primary objective is to reduce morbidity from influenza, then the morbidity-based and contact-based strategies are always preferred, although this advantage decreases as disease transmissibility (T) increases.

One might argue that the primary objective of intervention should be to reduce mortality rather than morbidity. The CDC's recent vaccine priorities seem to be based on this objective [12]. In terms of mortality, there is a specific transmissibility value below which the morbidity-based and contact-based strategies are superior and above which the mortality-based strategies are superior (Figure 4b). To clarify this transition (which occurs for our network at $T = 0.13$), we divide the adult and elderly subpopulations into infected, vaccinated, and uninfected in Figure 5. The uninfected class is made up of individuals that have neither been vaccinated nor get infected. Some of these individuals would not be infected in any case, and the rest are those that would be infected without a vaccination program but are now protected by the effects of herd immunity. Below the

transition point (for instance at $T = 0.1$), the elderly are protected more by the indirect effects of the morbidity-based strategy than by the direct effects of mortality-based strategy. Above the transition point (for instance at $T = 0.15$), the indirect protection by the morbidity-based strategy drops substantially, resulting in a higher proportion of elderly infected than with the mortality-based strategy. A similar reversal occurs for infants. The mixed strategy—a combination of morbidity-based and mortality-based strategies targets—is never the optimal strategy (Fig 4b), yet may be an advisable bed-hedging strategy when there is great uncertainty about the transmissibility of the circulating strain.

Estimates of R_0 for interpandemic flu range between 1 and 2 for the H2N2 and H3N2 type A strains of influenza [8,29]. Since influenza vaccines have been used in the United States since 1944, these estimates may be based on partially vaccinated populations. Conservatively assuming that the populations in question had somewhere between no coverage at all and 13% coverage according to the contact-based strategy, these values of R_0 ($1 < R_0 < 2$) correspond to $0.06 < T < 0.22$ in our model*. This range straddles the critical cross-points in Figures 4b and 4d, leaving some ambiguity as to which strategy will be most effective. We note, however, that the higher the transmissibility, the more dire the public health situation, and mortality-based strategies are predicted to be more effective for strains in the upper half of this estimated interval.

* Since R_0 is a product of both transmissibility (T) and the connectivity of the population, for a given value of T , different populations (networks) may have different values of R_0 . We derive the lower and upper bounds for T that correspond to $1 < R_0 < 2$ as follows. We take the value of T that yields $R_0 = 1$ for the population (network) with no vaccination (which is $T = 0.06$) and we take the value of T that yields $R_0 = 2$ for the population (network) with maximum (13%) vaccination coverage (which is $T = 0.22$).

Highly virulent influenza

The demographic-specific mortality rates reported for influenza vary considerably (Supporting Information). To assess whether control recommendations can be generalized to new or anomalous strains of influenza, we have analyze a second, extreme scenario. Worldwide influenza pandemics are characterized by much higher levels of morbidity and mortality than annual epidemics, and have occurred three times in the last century. The 1918-1919 “Spanish Influenza” caused more than 500,000 deaths in the United States and an estimated 20 million deaths worldwide [30]. Based on data from the 1918 pandemic, we modify our model in three respects: the number of people expected to seek medical attention upon infection, the age-specific mortality rates, and (consequentially) the age groups targeted by the mortality-based and mixed strategies.

Despite these substantial differences, the predictions for pandemic and interpandemic flu are qualitatively similar. The morbidity-based and contact-based strategies outperform mortality-based strategies in terms of resulting mortality for low values of T , but not for higher values. There is a quantitative difference, however, in that the transition point between these two regimes happens at a higher transmissibility for pandemic flu than interpandemic flu (Figure 4d vs. 4b). In other words, morbidity-based strategies are preferred for a wider spectrum of pandemic flu strains than interpandemic flu strains. This stems, in part, from the much larger size of the high-risk population (adults) for pandemic flu. Under vaccine limitations (13% in this case), the mortality-based strategy protects a much smaller fraction of the pandemic high-risk population than the interpandemic high-risk population. We have found that increasing the vaccination level to 20% (corresponding to the vaccine supply during 2004-2005 season [31]) does

not change the qualitative results (shown in the Supporting Information). Patel et al. have recently performed a similar sensitivity analysis for vaccine availability for a mildly transmissible strain of influenza A (H2N2) [32].

The reproductive number (R_0) for the 1918 Spanish Influenza is estimated to be between 1.8 and 4 [27,33], corresponding to T between 0.09 and 0.43 in our model (See footnote (*) above). These estimates fall in the range where mortality-based strategies are clearly more advisable than morbidity-based strategies (Figure 4d).

Multiple Introductions

Most communities do not exist in isolation, and thus experience multiple independent introductions of the virus during a typical flu season. Many models of vaccination strategies [8,9], however, ignore this possibility. For mathematical simplicity, we assume that multiple independent introductions occur simultaneously (and are chosen randomly) at the start of an outbreak, which yields conservative estimates of their detrimental impact. The probability of an epidemic increases with the number of introductions for all strategies, thereby reducing the advantage of the morbidity-based and contact-based strategies for mildly transmissible strains. For example, if there are four independent introductions of flu, morbidity-based strategies are inferior to mortality-based strategies above $T = 0.12$ ($R_0 = 2.1$). In contrast, this shift takes place at $T = 0.13$ ($R_0 = 2.3$), when there is a single importation of disease (Figure 6).

Delayed Intervention

A similar analysis provides insight into the impact of a delay in intervention until after an outbreak is already in progress, as occurred during the 2000-2001 flu season [34]. We simulate the implementation of vaccination after a certain proportion of the population has already been infected. We call this proportion “delay”. The morbidity-based strategies are more sensitive to such delays than mortality-based methods (Figure 7). They become inferior after $T = 0.11$ ($R_0 = 1.9$) if there is a 10% delay in vaccination, compared to $T = 0.13$ ($R_0 = 2.3$) when there is no delay.

Figures 6 and 7 suggest that a delay in vaccination may be less detrimental than multiple introductions of disease into a population. Multiple independent introductions of disease provide multiple independent opportunities to spark a large scale epidemic. In the absence of vaccination, the probability of an epidemic increases considerably as the number of independent introductions increase (Supporting Information). In contrast, a delay in vaccination allows a single case to grow into a connected cluster of cases, which are not independent of each other with respect to the numbers and the identities of their contacts. The probability of an epidemic increases with the number of individuals in the initial cluster, but not quickly as it does with the addition of independent cases.

CONCLUSION

In this study, we have applied the analytical methods of contact network epidemiology to evaluate current and proposed influenza vaccination priorities. In contrast to prior studies [9,32], we have modeled a relatively large population and the entire spectrum of viral transmission rates possible for influenza; in addition, we have accounted for multiple

introductions of disease and the possibility of a delay in vaccination. The efficacy of mortality-based strategies (like the CDC 2004 vaccination priorities [12]) and morbidity-based strategies (like school-based vaccination [8,9]) depend on (i) the transmissibility (reproductive number) of the strain; (ii) age-specific mortality rates; (iii) the vulnerability of the community to multiple introductions; and (iv) the timing of implementation. With respect to minimizing mortality, mortality-based strategies are generally preferred to morbidity-based strategies for strains with high transmission rates and in communities experiencing either delayed intervention or multiple introductions.

Thus, mortality-based strategies may be the prudent choice for outbreaks of new or atypical strains of influenza, when public health officials may not have reliable estimates for all (or any) of the first three inputs, and vaccination may be delayed. When reliable estimates of the key inputs are available significantly prior to an outbreak, this approach can be applied to design optimal (rather than just prudent) priorities. The predictions appear to hold for a range of age-specific mortality distributions estimated for past outbreaks of epidemic and pandemic flu. Although this suggests that similar recommendations may be appropriate for pandemic flu, they will be irrelevant in the very likely case that vaccines are not available at the start of an outbreak.

ACKNOWLEDGEMENTS:

The authors would like to thank Martin Meltzer, Robert C. Brunham, Mel Krajden, Danuta M. Skowronski, and James Lloyd Smith for their insightful suggestions; and acknowledge the financial support of the Canadian Institutes of Health Research, the Santa Fe Institute and a NASA Harriett G. Jenkins Fellowship to S.B. We also thank three anonymous referees for their valuable comments and suggestions.

AUTHOR CONTRIBUTIONS and COMPETING INTERESTS:

All three authors contributed to the design, analysis and presentation of this work. The authors declare no competing financial interests.

REFERENCES:

1. Govaert, T.M.E., et al. The efficacy of influenza vaccination in elderly individuals. *JAMA* **272**, 1661-1665 (1994)
2. Brandriss, M.W., Betts, R.F., Mathur, U., Douglas, R.G. Jr. Responses of elderly subjects to monovalent A(H1N1) and trivalent A(H1N1)/A(H3N2)/B vaccines. *Am. Rev. Resp. Dis.* **124**, 681-684 (1981)
3. Longini, I.M., Koopman, J.S., Monto, A.S., Fox, J.P. Estimating household and community transmission parameters of influenza. *Am J Epidemiol* **115**, 736-51 (1982)
4. Fox, J.P., Hall, C.E., Cooney, M.K., Foy, H.M. Influenza virus infections in Seattle families, 1975-1979. *Am. J. Epidemiol.* **116**, 212-27 (1982)
5. Jennings, L.C., Miles, J.A.R. A study of acute respiratory disease in the community of Port Chalmers. *J. Hyg. (London)* **81**, 67-75 (1978)
6. Taber, L.H., Paredes, A., Glezen, W.P., Couch, R.B. Infection with influenza A/Victoria virus in Houston families, 1976. *J. Hyg. (Lond)* **86**, 303-13 (1982)
7. Glezen, W.P. Emerging infections: pandemic influenza. *Epidemiol. Rev.* **18(1)**, 64-76 (1996)
8. Longini, I.M. Jr., Halloran, M.E., Nizam, A., Yang Y. Containing pandemic influenza with antiviral agents. *Am. J. Epidemiol.* **159**, 623-33 (2004)
9. Longini, I.M., Halloran, M.E. Strategy for Distribution of Influenza Vaccine to High-Risk Groups and Children. *Am. J. Epidemiol.* **161**, 303-306 (2005)
10. Monto, A.S., Koopman, J.S., Longini, I.M. Jr. The Tecumseh study of illness. XIII. Influenza infection and disease. *Am. J. Epidemiol.* **121**, 811-22 (1985)
11. Reichart, T.A., et al. The Japanese experience with vaccinating school-children against influenza. *N. Engl. J. Med.* **344**, 889-96 (2001)
12. Centers for Disease Control and Prevention. Prevention and control of influenza: recommendations of the Advisory Committee on Immunization Practices (ACIP). *MMWR* **53**, No. RR-6 (2004)
13. Dezsó, Z., Barabási A.-L., Halting viruses in scale-free networks. *Phys. Rev. E* **65**, 055103 (2001)
14. Pastor-Satorras, R., Vespignani, A., Immunization of complex networks. *Phys. Rev. E* **65**, 036104 (2001)

15. Meyers, L.A., Newman, M.E.J., Martin, M., Schrag, S. Applying network theory to epidemics: control measures for *Mycoplasma pneumoniae* outbreaks. *Emerg. Infect. Dis.* **9**, 204 (2003)
16. Meyers, L.A., Pourbohloul, B., Newman, M.E.J., Skowronski, D.M., Brunham, R.C. Network Theory and SARS: predicting outbreak diversity. *JTB* **232**, 71-81 (2005)
17. Pourbohloul, B. et al. Modeling Control Strategies of Respiratory Pathogens. *Emerg. Infect Dis.* **11 (8)**, 1249-1256 (2005)
18. Thompson, W.W., Shay, D.K., Weintraub, E. Influenza-associated hospitalizations in the United States. *JAMA* **292**, 1333-1340 (2004)
19. Paul, Y. Herd Immunity and Herd protection. *Vaccine*. **22(3-4)**, 301-2 (2004)
20. Interim Estimates of Populations Targeted for Influenza Vaccination From 2002 National Health Interview Survey Data and Estimates for 2004 Based on Influenza Vaccine Shortage Priority Groups, Centers for Disease Control. (2004).
21. Thompson, W.W. et al. Mortality associated with influenza and respiratory syncytial virus in the United States. *JAMA* **289**, 179–86 (2003)
22. Simonsen L. et al. Pandemic versus epidemic influenza mortality: a pattern of changing age distribution. *J. Infect. Dis.* **178**, 53–60 (1998)
23. Dauer, C.C., Serfling, R.E. Mortality from influenza, 1957-1958 and 1959-1960. *Am. Rev. Respir. Dis.* **83 (Suppl 2)**, 15-26 (1961)
24. Olsen, D.R., Simonsen, L., Edelson, P.J., Morse, S.S. Epidemiological evidence of an early wave of the 1918 influenza Pandemic in New York City. *PNAS* **102**, 11059-63 (2005)
25. Newman, M.E.J. Spread of epidemic disease on network. *Phys. Rev. E* **66**, 016128 (2002)
26. Meyers, L.A., Newman, M.E.J., Pourbohloul, B. Predicting epidemics on directed contact networks. *JTB* – In press (2005)
27. Frost, W.H. Statistics of influenza morbidity: with special reference to certain factors in case incidence. *Public Health Reports* **36**, 584-97 (1920)
28. Ferguson, N.M., Cummings, D.A.T., Cauchemez, S., et al. Strategies for containing an emerging influenza pandemic in Southeast Asia. *Nature* **437**, 209-14 (2005)

29. Hethcote, H.W. The mathematics of infectious diseases. *SIAM Review* **42** (4), 599-653 (2000)
30. Noble, G.R. Epidemiological and clinical aspects of influenza. In: Beare, A.S., ed. *Basic and Applied Influenza Research*. Boca Raton, FL: CRC Press, 11–50 (1982)
31. Centers for Disease Control and Prevention. Interim Influenza Vaccination Recommendations, 2004-2005 Influenza Season. *MMWR* **53** (Dispatch):1 (Oct 5, 2004)
32. Patel, R., Longini, I.M., Halloran, M.E. Finding optimal vaccination strategies for pandemic influenza using genetic algorithms. *JTB* **234**, 201-212 (2005)
33. Mills, C.E., Robins, J.M., Lipsitch, M. Transmissibility of 1918 pandemic influenza. *Nature* **432**, 904-906 (2004)
34. Flu Vaccine Supply, Flu Season 2001, CDC, Division of Media Relations, June 2000, <http://www.cdc.gov/od/oc/media/pressrel/r2k0622a.htm> (accessed March 25, 2005)
35. Woolhouse, M. E. et al. Heterogeneities in the transmission of infectious agents: implications for the design of control programs. *PNAS* **94**, 338-342 (1997)
36. Cauchemez, S., Carrat, F., Viboud, C., Valleron, A.J., Boelle, P.Y. A Bayesian MCMC approach to study transmission of influenza: application to household longitudinal data. *Stat Med* **23** 3469-3487

	Vaccination Coverage Levels	Inactivated Vaccine Efficacy
Infants (6 m - 3 yrs)	30-75%	70-90%
Toddlers (3 - 5 yrs)	30-75%	70-90%
Children(5 - 18 yrs)	30-75%	77-91%
Adults (18 - 50 yrs)	30-75%	70-90%
Elders (> 50 yrs)	67-85%	30-50%
Health Care Workers	25-38%	70-90%
Elders in Care Facilities	90-95%	30-50%

Table 1: Historical influenza vaccination coverage levels and inactivated vaccine efficacy levels used in this study^{12, 30}.

	Implemented Coverage Level	Vaccine Efficacy	Effective Coverage Level
Infants (6m-3)	75% (4.1% of total population)	90%	68%
Elders (>50)	85% (7.5% of total population)	50%	43%
Health Care Workers	38% (0.4% of total population)	90%	34%
Elders in Care Facilities	95% (0.7% of total population)	50%	48%
TOTAL	12.7% of total population		

Table 2: Vaccination coverage and efficacy levels assumed for the mortality-based vaccination strategy. The effective coverage level is a product of the implemented coverage level and vaccine efficacy for each group.

	Mortality Rate Influenza Epidemic (per 10,000 cases)	Mortality Rate Influenza Pandemic (per 10,000 cases)
Infants (6 m - 3 yrs)	0.30	80.0
Toddlers (3 - 5 yrs)	0.08	50.0
Children(5 - 18 yrs)	0.08	20.0
Adults (18 - 50 yrs)	0.07	70.0
Elders (> 50 yrs)	12.00	5.0

Table 3: The age-specific mortality distributions for typical annual influenza epidemics and an example influenza pandemic.

FIGURES:

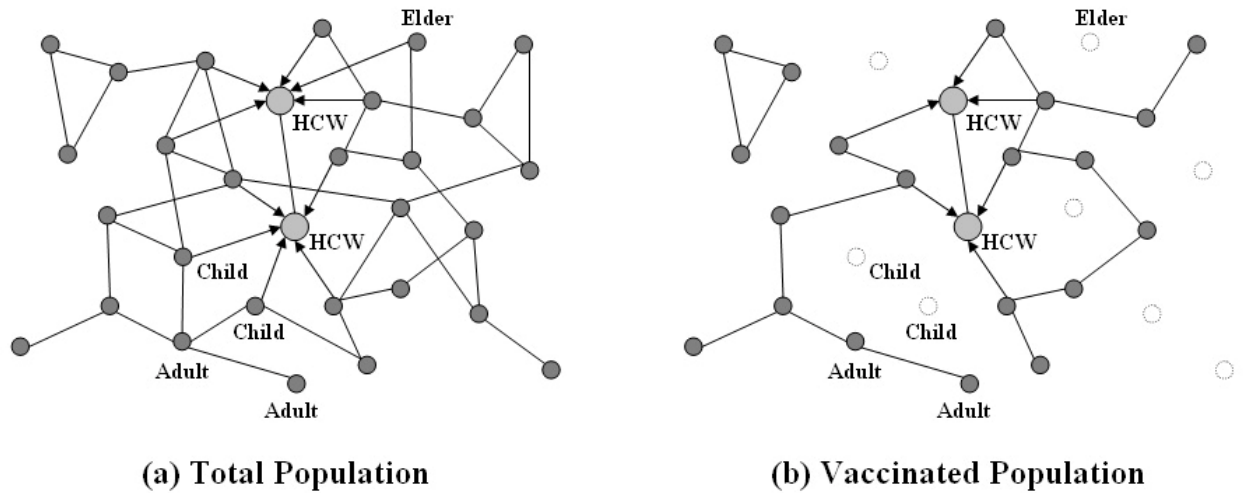


Figure 1: Network Model

(a) A schematic of a network model for an urban population. Each individual is a vertex in the network, and edges represent potentially disease-causing contacts between individuals. Directed edges (with arrows) represent transmission occurring in only one direction. (b) We model vaccination in a population by removing nodes from the population network, and the edges that are attached to them.

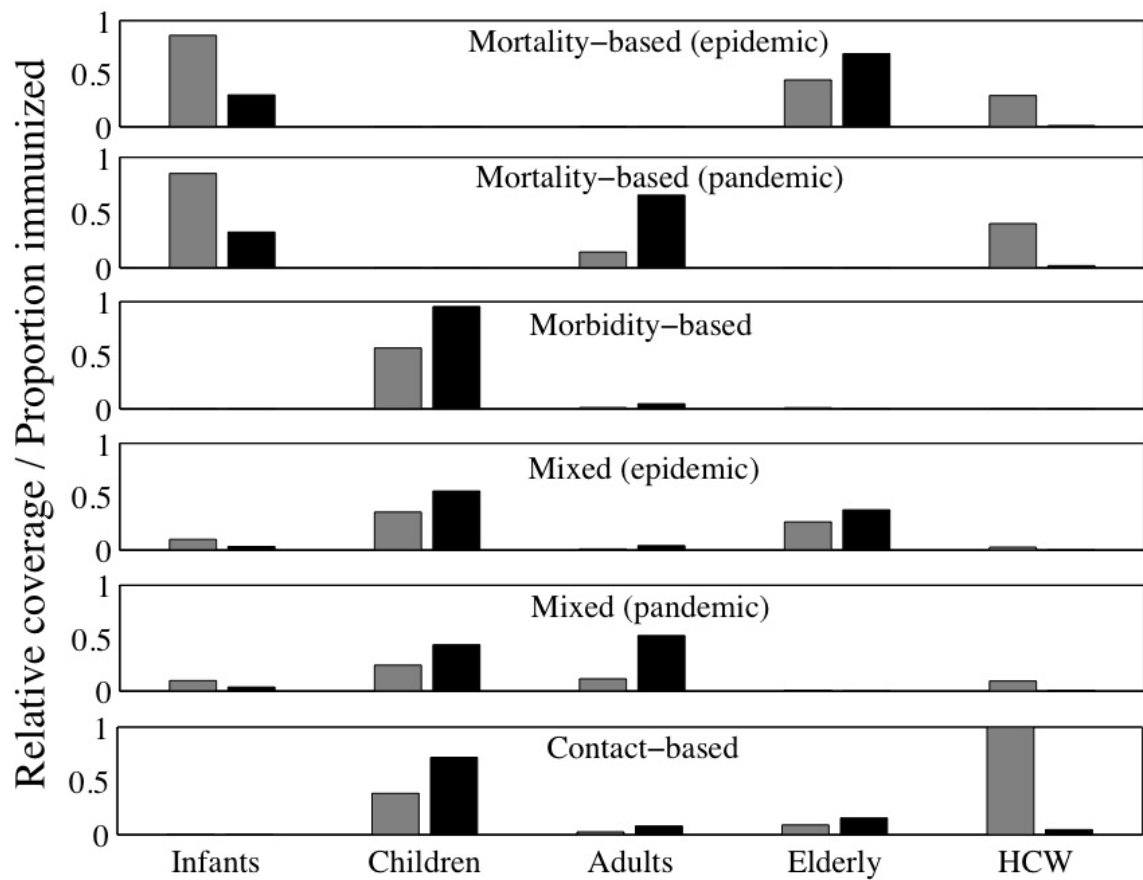


Figure 2: Vaccination Strategies

The demographic distribution of vaccines according to each of the strategies: the black bars reflect the fraction of available vaccines given to each age group (and thus will always sum to one.) The gray bars reflect the proportion of each demographic that is effectively immunized, and thus take into account the size of the demographic and the demographic-specific vaccine efficacy.

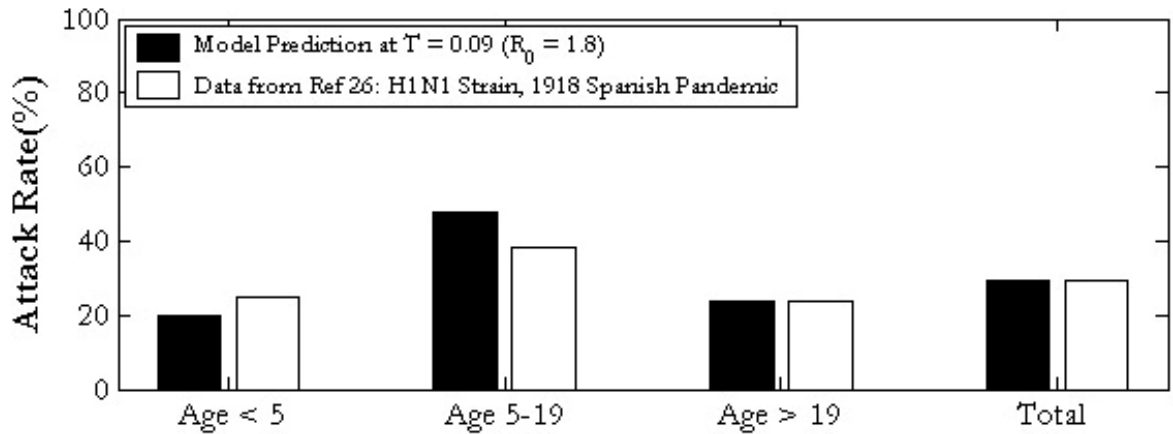


Figure 3: Model Validation

Comparison of age-specific attack rate data for the 1918 influenza pandemic between data reported in literature and our model predictions. The differences between the model predictions and the data may result from discrepancies between the demographic profile of a typical urban population today and that of 1918.

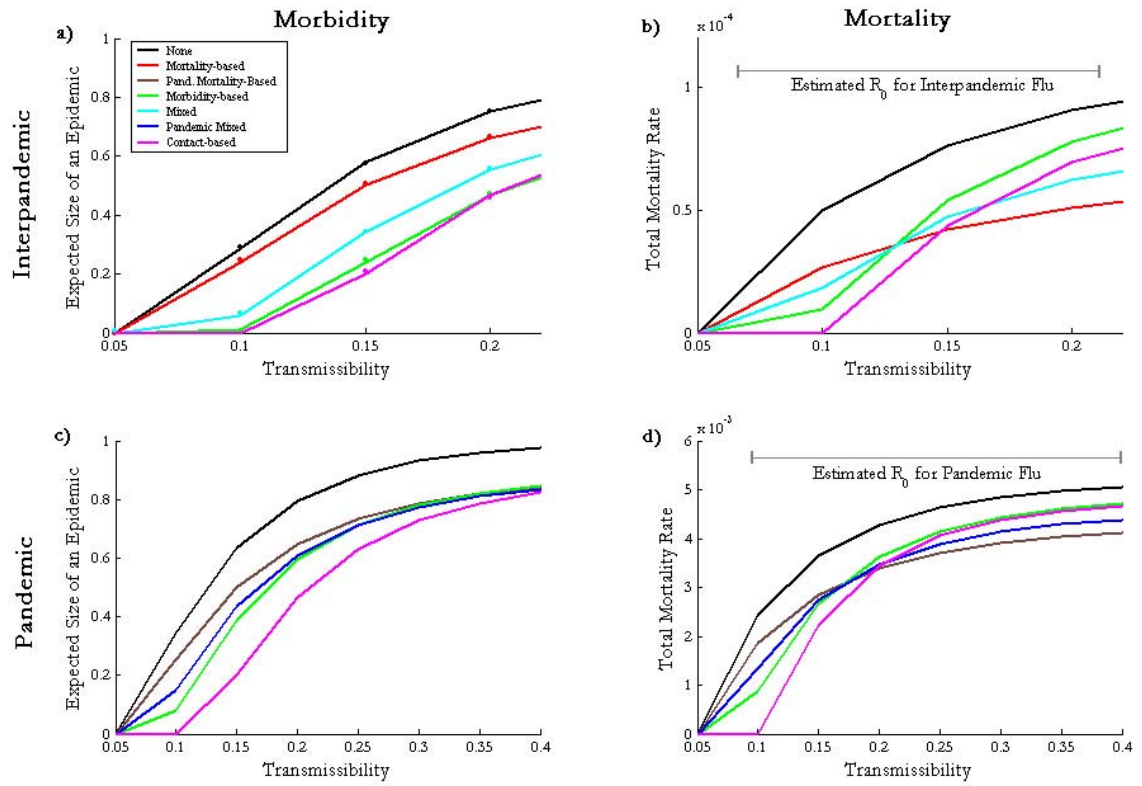


Figure 4: Morbidity and mortality for influenza epidemics and pandemics

(a) Expected attack rate and (b) mortality rate as a function of T for annual influenza epidemics.

(c) Expected attack rate and (d) mortality rate as a function of T for an influenza pandemic.

The dots on (a) show simulation results for comparison. Estimates of R_0 for interpandemic and pandemic flu are shown as gray lines in (b) and (d), respectively.

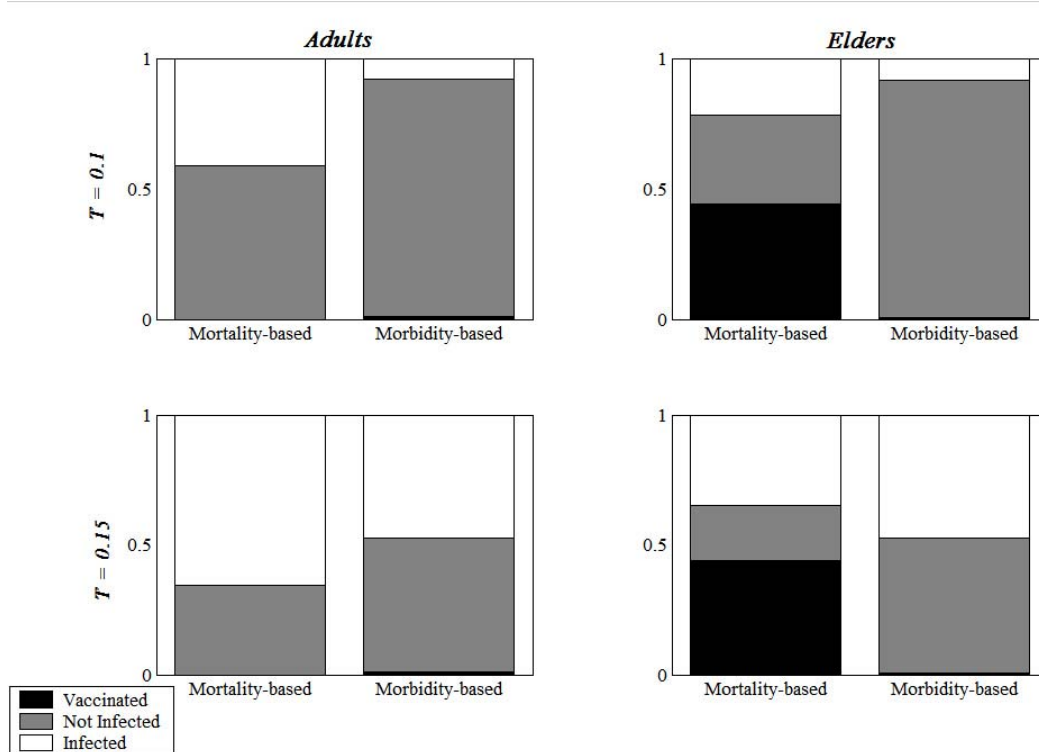


Figure 5: Direct vs. indirect intervention

The adult and elderly populations are divided into infected, protected (not vaccinated or infected) and vaccinated for two different values of R_0 , and for both the mortality-based and mixed strategies.

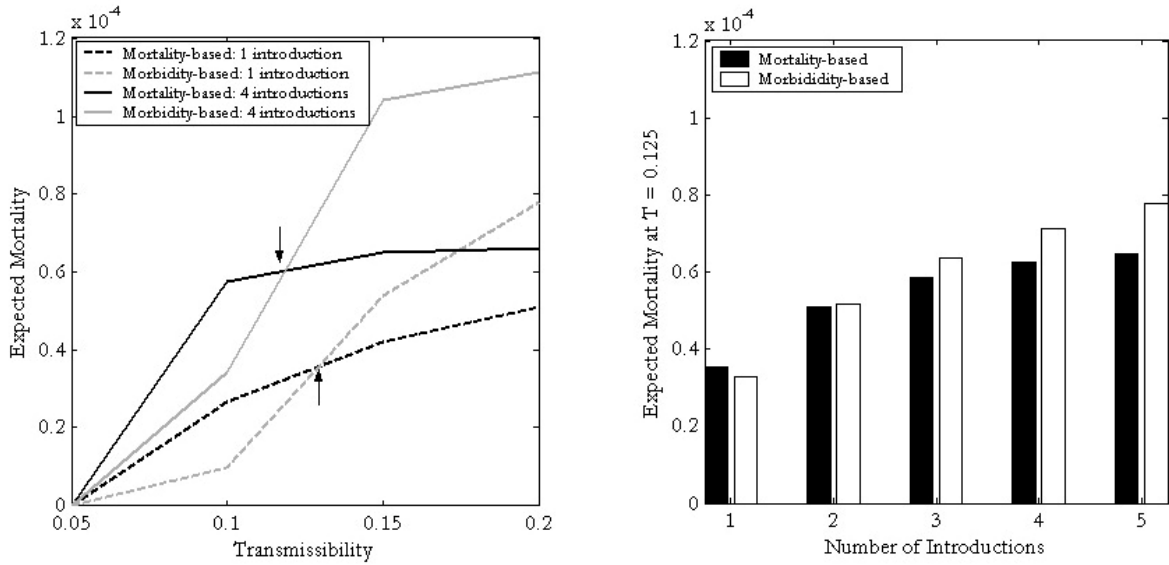


Figure 6: The epidemiological impact of multiple introductions of disease

(a) The morbidity-based strategy is more effective than the mortality-based strategy when $T < 0.13$ if there is only single introduction of disease, yet it becomes relatively less effective (preferred when $T < 0.12$) when there are four introductions of the disease. (b) At $T = 0.125$, the morbidity-based strategy is superior to mortality-based strategy when there is a single introduction, but inferior when there is more than one introduction.

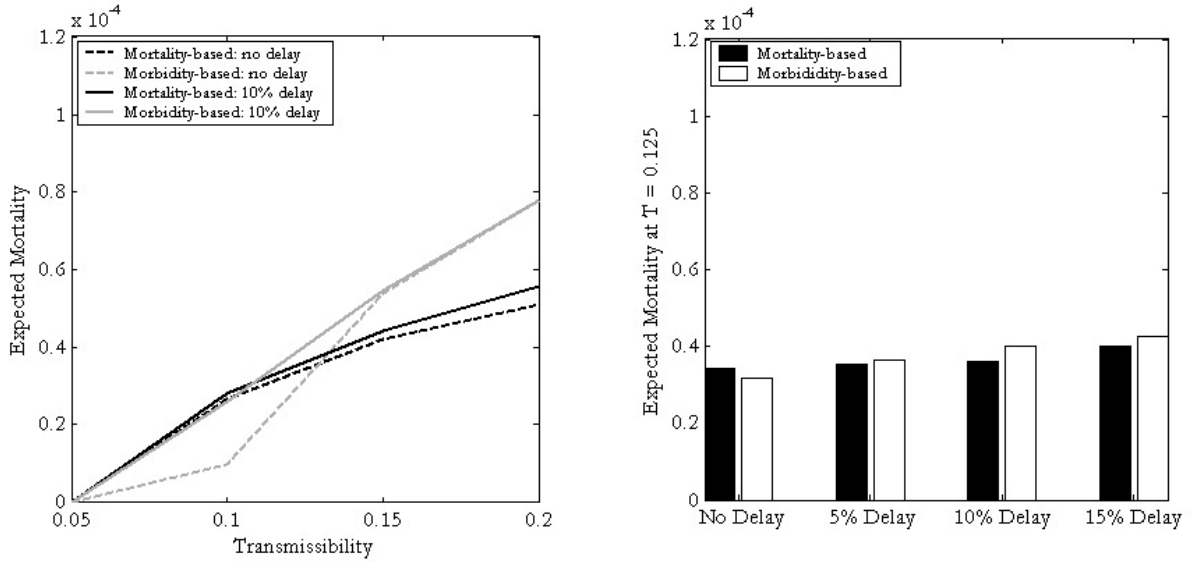


Figure 7: The epidemiological impact of delayed vaccination

(a) The morbidity-based strategy is more effective than the mortality-based strategy when $T < 0.13$ if there is no delay in vaccination, yet it becomes relatively less effective (preferred when $T < 0.11$) when vaccines are given after 10% of the population has already been infected. (b) At $T = 0.125$, the morbidity-based strategy is superior to mortality-based strategy when there is no delay, but inferior for any amount of delay. Each of the values is an average taken across 500 epidemic simulations on the contact network.

Supporting Information:

Quantitative Comparison of Influenza Vaccination Programs

Shweta Bansal, Babak Pourbohloul, Lauren Ancel Meyers

SUPPLEMENTAL METHODS

Urban Contact Network Generation

In our study, we generate a plausible contact network for an urban setting using demographic information for the Greater Vancouver Regional District, which is the third largest metropolitan area in Canada. We use publicly available data from sources such as Statistics Canada to estimate the distribution of ages, household sizes, school and classroom sizes, hospital occupancy, workplaces, and public spaces [S1-S4].

Qualitatively similar age and household size distributions are found for other cities in Canada ranging in population sizes from 120,000 to 4.6 million [S5]. We begin assembling the urban network by choosing 100,000 households at random from the Vancouver household size distribution [S1], which yields approximately 257,000 people according to a mean household size of approximately 2.6. Based on ages assigned from the measured Vancouver age distribution [S2], each member of the population is assigned to an activity: to schools according to school and class size distributions [S3]; to occupations according to (un)employment data; to hospitals as patients and caregivers according to hospital employment and bed data [S4]; to nursing homes according to nursing home occupancy data; and to other public places.

To model heterogeneities in contact patterns, we create random connections (edges) between individuals (nodes) based on the location and nature of their overlapping daily activities. Individuals in households are connected with probability 1, while

individuals encountering others in public places are connected with probabilities ranging from 0.003 to 0.3. Each school and hospital is subdivided into classrooms or wards. Pairs of students and pairs of patients within these subunits are connected with higher probability than pairs associated with different subunits. Teachers are assigned to classrooms and connected stochastically to appropriate students. Caregivers are assigned wards and then connected to appropriate patients. There are also low probability neighborhood contacts between individuals from different households.

Epidemiological Analysis

The methods described in this section are derived and described fully in Ref S6. Here, we only present the expressions with a few motivating details. The network in our model is a *semi-directed* one as it has undirected and directed edges. A semi-directed network, each vertex (individual) has an *undirected-degree* representing the number of undirected edges joining the vertex to other vertices as well as both an *in-degree* and an *out-degree* representing the number of directed edges coming *from* other vertices and going *to* other vertices, respectively. The undirected-degree and in-degree indicate how many contacts can spread disease to the individual, and thus is related to the likelihood that an individual will become infected during an epidemic; and the undirected-degree and out-degree indicate how many contacts may be infected by that individual should he or she become infected, and thus is related to the likelihood that an individual will ignite an epidemic.

Given the degree distribution of the contact network within a population, one can analytically predict what will happen when an infectious disease like influenza

enters the population. Let p_{jkm} be the probability that any given person in the population has in-degree equal to j , out-degree equal to k , and undirected-degree m . Let T be the transmissibility of the disease, that is, the average probability that transmission of the disease occurs between an infected individual and a susceptible individual with whom they are in contact.

Network theory makes a technical distinction between outbreaks and epidemics. An outbreak is a causally connected cluster of cases which, by chance or because the transmission probability is low, dies out before spreading to the population at large. In an epidemic, on the other hand, the infection escapes the initial group of cases into the community at large and results in population-wide incidence of the disease. The crucial difference is that the size of an outbreak is determined by the spontaneous dying out of the infection, whereas the size of an epidemic is limited only by the size of the population through which it spreads.

To predict the fate of an outbreak, we use *probability generating functions*, to summarize useful information about network topology. Thus, if a graph has degree distribution p_{jkm} , then the probability generating function (PGF, henceforth) for p_{jkm} is

$$\Gamma(x, y, u) = \sum_{jkm} p_{jkm} x^j y^k u^m .$$

The average in-degree, out-degree, and undirected-degree are equal to:

$$\langle k_{in} \rangle = \sum_{jkm} j p_{jkm} , \langle k_{out} \rangle = \sum_{jkm} k p_{jkm} , \text{ and } \langle k_{un} \rangle = \sum_{jkm} m p_{jkm} .$$

The average degrees can

also be expressed by evaluating the partial derivatives of $\Gamma(x, y, u)$ at

$x = 1, y = 1$ and $u = 1$. We note that since every directed edge has an origin and a destination, the average in-degree equals the average out-

$$\text{degree} \left(\sum_{jkm} jp_{jkm} = \sum_{jkm} kp_{jkm} = \sum_{jkm} \frac{j+k}{2} p_{jkm} \right).$$

If you choose a random *directed* edge in the network and follow it to the nearest vertex, then the PGF for the number of the three types of edges (in, out, and undirected) emanating from that vertex other than the one that we arrived on is

$$H_d(x, y, u) = \frac{\sum_{jkm} jp_{jkm} x^{j-1} y^k u^m}{\langle k_{in} \rangle}.$$

Likewise, if you choose a random *undirected* edge in the network and follow it to the nearest vertex, then the PGF for the various edges at that vertex is given by

$$H_u(x, y, u) = \frac{\sum_{jkm} mp_{jkm} x^j y^k u^{m-1}}{\langle k_{un} \rangle}.$$

Using these methods, we can derive the reproductive ratio, R_0 , the average size of an outbreak, $\langle s \rangle$, the size of an epidemic, S_e , the probability of an epidemic, P_e , and the probability that an individual with a certain (in- and undirected-) degree will get infected, v_{jm} .

The basic reproductive ratio: When calculating the expected number of new cases arising from an infection in a naïve population we consider the source vertex of the infection. That is, the initial case may arise through infection along a directed or undirected edge. Thus, if we know the source of the infection we can more accurately

predict the R_0 . In particular, $R_0^d = T \frac{\sum_{jkm} j(k+m)p_{jkm}}{\langle k_{in} \rangle}$ and $R_0^u = T \frac{\sum_{jkm} m(k+m-1)p_{jkm}}{\langle k_{un} \rangle}$

respectively, where T is the average disease transmissibility and the second term is the average out-degree plus the average undirected-degree of a vertex that has become infected along a randomly selected edge. When we do not know anything about the transmission event that led to the initial infection, then our best estimate is

$$R_0 = T \frac{\sum_{jkm} (j(k+m) + m(k+m-1)) p_{jkm}}{\langle k_{in} \rangle + \langle k_{un} \rangle}.$$

The average size of small outbreaks and the epidemic threshold: By nesting PGFs for the number of new infections emanating from an infected vertex one can construct a PGF for the size of a small outbreak, and hence derive the average size of a small outbreak:

$$\langle s \rangle = 1 + \frac{T f_1^j [1 - T(f_m^{m(m-1)} - f_j^{jm})] + T f_1^m [1 - T(f_j^{jk} - f_m^{km})]}{(1 - T f_j^{jk})(1 - T f_m^{m(m-1)}) - T^2 f_j^{jm} f_m^{km}}$$

where $f_b^a = \frac{\sum_{jkm} a p_{jkm}}{\sum_{jkm} b p_{jkm}}$. When T is small, the average size of a small outbreak is

finite, but $\langle s \rangle$ grows with increasing transmissibility, until it diverges when the denominator of the expression above reaches its first zero. This point marks the phase transition at which the typical outbreak ceases to be confined to a finite number of cases and expands to a large-scale epidemic covering most of the network. This transition happens when T is equal to the critical transmissibility T_c , given by

$$T_c = \frac{(f_j^{jk} + f_m^{m(m-1)}) \pm \sqrt{(f_j^{jk} + f_m^{m(m-1)})^2 - 4(f_j^{jk} f_m^{m(m-1)} - f_j^{jm} f_m^{km})}}{2(f_j^{jk} f_m^{m(m-1)} - f_j^{jm} f_m^{km})}.$$

The expected size of a full-blown epidemic S_e : We can compute the size of the epidemic, S_e , for the case when T is larger than T_c . We first calculate the likelihood that infection of a randomly chosen individual will spark only a limited outbreak instead of a full-blown epidemic, and then take one minus that probability:

$$S_e = 1 - \sum_{jkm} p_{jkm} (1 + (a-1)T)^j (1 - (b-1)T)^m,$$

where a and b are the solutions to the self-consistent equations

$$a = \frac{\sum_{jkm} k p_{jkm} (1 + (a-1)T)^j (1 + (b-1)T)^m}{< k_{out} >} \quad \text{and} \quad b = \frac{\sum_{jkm} m p_{jkm} (1 + (a-1)T)^j (1 + (b-1)T)^{m-1}}{< k_{un} >}. \quad \text{We}$$

use numerical root finding methods (such as Newton's method) to solve for a and b .

The probability of a full-blown epidemic P_e : The expression for P_e comes from first calculating the likelihood that a single infection will lead to only a small outbreak instead of a full-blown epidemic, and then and then taking one minus the probability:

$$P_e = 1 - \sum_{jkm} p_{jkm} (1 + (\alpha-1)T)^k (1 - (\beta-1)T)^m,$$

where α and β are the solutions to the self-consistent equations

$$\alpha = \frac{\sum_{jkm} j p_{jkm} (1 + (\alpha-1)T)^k (1 + (\beta-1)T)^m}{< k_{in} >} \quad \text{and} \quad \beta = \frac{\sum_{jkm} m p_{jkm} (1 + (\alpha-1)T)^k (1 + (\beta-1)T)^{m-1}}{< k_{un} >}. \quad \text{We}$$

use numerical root finding methods (such as Newton's method) to solve for α and β .

The probability that an individual will be infected during an epidemic v_{jm} : The likelihood that an individual of in-degree j and undirected-degree m will be infected during an epidemic is equal to one minus the probability that none of his or her $j + m$ contacts will transmit the disease to him or her. The probability that a contact does not transmit the disease is equal to the probability that the contact was infected, but did not transmit the disease, $1 - T$, plus the probability that the contact was not infected in the first place, Ta for the directed edges, Tb for the undirected edges. Thus, a randomly chosen vertex of in-degree j and undirected-degree m will become infected with probability

$$v_{jm} = 1 - (1 - T + Ta)^j (1 - T + Tb)^m .$$

Demographic-Specific Attack Rates: We calculate demographic-specific epidemiological risks by combining demographic information (age, occupation, etc.) for each member of the population with the v_{jm} , defined above. We first divide the population into 14 demographic groups:

<i>Demographic Group (g)</i>	<i>Demographic Group Description</i>
1	Infants (age < 3)
2	Toddlers (3 ≤ age < 5)
3	Children (5 ≤ age < 18)
4	Adults (18 ≤ age < 50)
5	Elderly (age > 50)
6	Nursing home residents
7	Infants in daycare
8	Toddlers in preschool
9	Health care workers
10	Nursing home workers
11	Day care workers
12	Preschool workers

13	Teachers (and school staff)
14	Unemployed

For each demographic group (g), we find the number of infections (N_g) at a particular transmission probability T by aggregating the probabilities of infection (v_{jm}) for each individual (i) with in-degree $j(i)$ and undirected degree $m(i)$:

$$N_g = \sum_{i \in g} v_{j(i)m(i)} \quad \forall g \in [1,14]$$

Age-Specific Mortality: The predicted number of deaths in the population caused by an epidemic (M) is the product of the predicted number of infections in each of the age groups (N_g for all g in $[1,5]$) and the age-specific mortality rate (R_g) specified in

Table 3:

$$M = \sum_{g=1}^5 N_g * R_g$$

The predicted total mortality rate for the population is M normalized by the population size.

Multiple Introductions: We can also analytically predict the probability of an epidemic given multiple introductions of disease into a population. For a given number of introductions, n , the probability of an epidemic is given by:

$$\pi_n = 1 - (1 - P_e)^n,$$

where, P_e , is the probability of an epidemic assuming a single introduction. We note that the calculation of π_n above assumes that all n introductions occur independently at

the outset of an outbreak. This assumption yields a lower bound estimate for the probability of an epidemic with multiple introductions.

Epidemic Simulation

We verify the analytic predictions using simulations of a Susceptible-Infectious-Recovered (SIR) model. The simulations are initialized with an entirely susceptible population, except for a single infected case (*patient zero*). An infected vertex passes the disease on to each of its neighbors (those with whom that individual has disease-causing contacts) with probability T (the average transmission probability). This process continues until the population no longer includes any susceptible individuals that are in contact with any infected individuals. Once an individual has had the chance to infect its neighbors, it is immediately moved into the recovered class.

SUPPLEMENTAL ANALYSIS

Network Properties of Demographic Groups

Here we describe basic properties of the simulated urban networks that we have analyzed. The epidemiological calculations consider the degree distribution of the network (as described in the previous section.) Recall that most of the edges in our network are undirected and many individuals have the same out-degree as in-degree, with the exception of health care workers and individuals who are at high risk for complications due to flu. In Figure S1, we show the in-degree distributions for the total population and select demographic groups before and after vaccination by the morbidity and mortality-

based strategies. Children have a much higher mean in-degree (24.1) than adults and elders (10.7 and 10.6, respectively). Figure S1c illustrates that the contact patterns for adults are relatively unaffected by both the morbidity- and mortality-based strategies. The morbidity-based strategy primarily alters the degree distribution of children (Fig S1b) and the mortality-based strategy primarily alters the degree distribution of elders (Fig S1d).

Sensitivity to Population Structure

The urban networks are stochastically generated, yielding Poisson distributions of contact numbers within each setting (schools, hospitals, workplaces, etc.). To achieve this, we specify setting-specific probabilities that determine whether or not any given pair of individuals in the same location will have an edge drawn between them. We examined the sensitivity of our results to the specific probabilities used in generating the network. First, we generate 100 networks each with 5000 households. (The smaller population size allowed for more extensive sensitivity analyses. In prior studies, we found that epidemiological predictions for small urban networks apply to large urban networks [S5], and thus we expect that these sensitivity results will also apply to large networks.) To generate variation in these networks, we draw contact probabilities between individuals from a Gaussian distribution, and allow them to deviate by up to 15% from the original contact parameters (which range from 0.003 to 0.3 depending on the location/nature of the interaction). The stochastic formation of edges according to these probabilities yields 100 unique networks, each with its own degree distribution. We then vaccinate each population according to the morbidity-based and mortality-based strategies, as described

in the methods section. The dashed lines in Figure S2 indicate the standard deviations for each epidemiological prediction (morbidity and mortality) across the 100 networks. The minimal variation in the predictions indicates that our results are robust to stochastic variation in network structure. Even with a 15% deviation in contact structure, the morbidity and mortality-based strategies are superior for lower and higher values of T , respectively. The value of T at which the advantage of the morbidity-based strategy reduces falls in the range $[0.10, 0.12]$. In the main text, we report $T=0.11$ as the value where this advantage reduces. These results show that there is an uncertainty of 0.01 around that reported value.

Sensitivity to Variation in Mortality Rates and Distribution

To evaluate the sensitivity of our predictions to variations in virulence among different strains of influenza, we evaluated vaccination strategies for two markedly different estimated mortality distributions. Here we extend this analysis to several other estimated influenza mortality distributions. We compare the total mortality caused by an influenza epidemic after the population has been vaccinated with a morbidity-based or mortality-based strategy for five different age-specific mortality distributions. The first two mortality distributions are the focus of the main text. The third is a differing distribution for the 1918 pandemic with high mortality rates for adults and the elderly; and the remaining two are U-shaped mortality distributions from the epidemics of 1892 and 1936 [S8]. The mortality-based strategy is designed to target the demographic groups with the highest mortality rates, and thus varies from one mortality distribution to the next. The morbidity-based strategy is identical across all five mortality distributions, targeting

school children and staff as specified in the main text. We are particularly interested the cross-points (in transmissibility values) where the mortality-based strategy becomes superior to the morbidity-based strategy. These lie between $T = 0.15$ and $T = 0.20$ for the three additional mortality distributions shown in Fig S3, very close to that predicted for the 1918 mortality distribution considered in the main text, further suggesting that the results are fairly insensitive to uncertainties in mortality associated with pandemic influenza.

Sensitivity to Vaccine Coverage Level

We test the sensitivity of our results to a change in the vaccine coverage level. The vaccine priorities in the main text are implemented at a 13% coverage level. Here, we implement the morbidity-based strategy (school children and staff) and mortality-based strategy (based on the second mortality distribution of Fig S3) at a 20% coverage level. (During the influenza vaccine shortage of 2004, enough vaccine was available to cover 20% of the population.) Fig S4 shows that the increase in vaccination coverage produces a smaller mortality rate for both strategies but the comparison is qualitatively similar: the mortality-based strategy outperforms the morbidity-based strategy for higher values of transmissibility.

Sensitivity to Variation in Infectivity and Susceptibility

There is certainly heterogeneity in influenza infectivity and susceptibility among individuals. Some of the heterogeneity is caused by variation in contact patterns [S9]. Individuals with more contacts will have greater opportunities to catch and spread

disease. Our models explicitly capture this source of variation. The remaining heterogeneity in transmission rates is caused by intrinsic physiological and behavioral differences among individuals. Our analytical calculations allow for such heterogeneity so long as it is distributed somewhat randomly with respect to the structure of the population. That is, there should not be significant correlations between individual contact patterns and individual likelihoods of infection and/or transmission. There is evidence, however, that such correlations may exist. Cauchemez et al. statistically argue that children have a 50% higher infectiousness and about a 15% higher susceptibility than adults *per contact* [S10].

We have modified our contact network to model explicitly this diversity in transmissibility. Every individual in the network is assigned an infectivity value and a susceptibility value, and the probability of transmission along an edge is then calculated as the product of the infectivity of the infected individual and the susceptibility of the uninfected individual. As suggested by Cauchemez et al., children are assumed to have infectivity values 50% higher than that of adults ($J_{\text{child}} = 1.5 \cdot J_{\text{adult}}$) and susceptibility values 15% higher than that of adults ($S_{\text{child}} = 1.15 \cdot S_{\text{adult}}$). All individual infectivity and susceptibility values are chosen from Gaussian distributions with the appropriate means (J_{adult} , J_{child} , S_{adult} , S_{child} , etc.) In Figure S5, we give the results of 250 SIR simulations of influenza transmission through these networks with and without vaccination. Our current analytic methods give qualitatively similar, though not quantitatively similar results. The analytic methods described in the earlier sections can easily be extended to account for correlations in individual transmissibility, although this is beyond the scope of this paper.

In Fig S5, we see that the higher transmissibility values for children cause the mortality-based strategy (red) to be superior for an even larger range of strains than when there is no variation in transmissibility (Fig 4b). Although the morbidity-based strategy is now targeting the most infectious and vulnerable individuals in the population (school children), an even larger proportion of that group is required to be vaccinated to achieve the same amount of herd immunity.

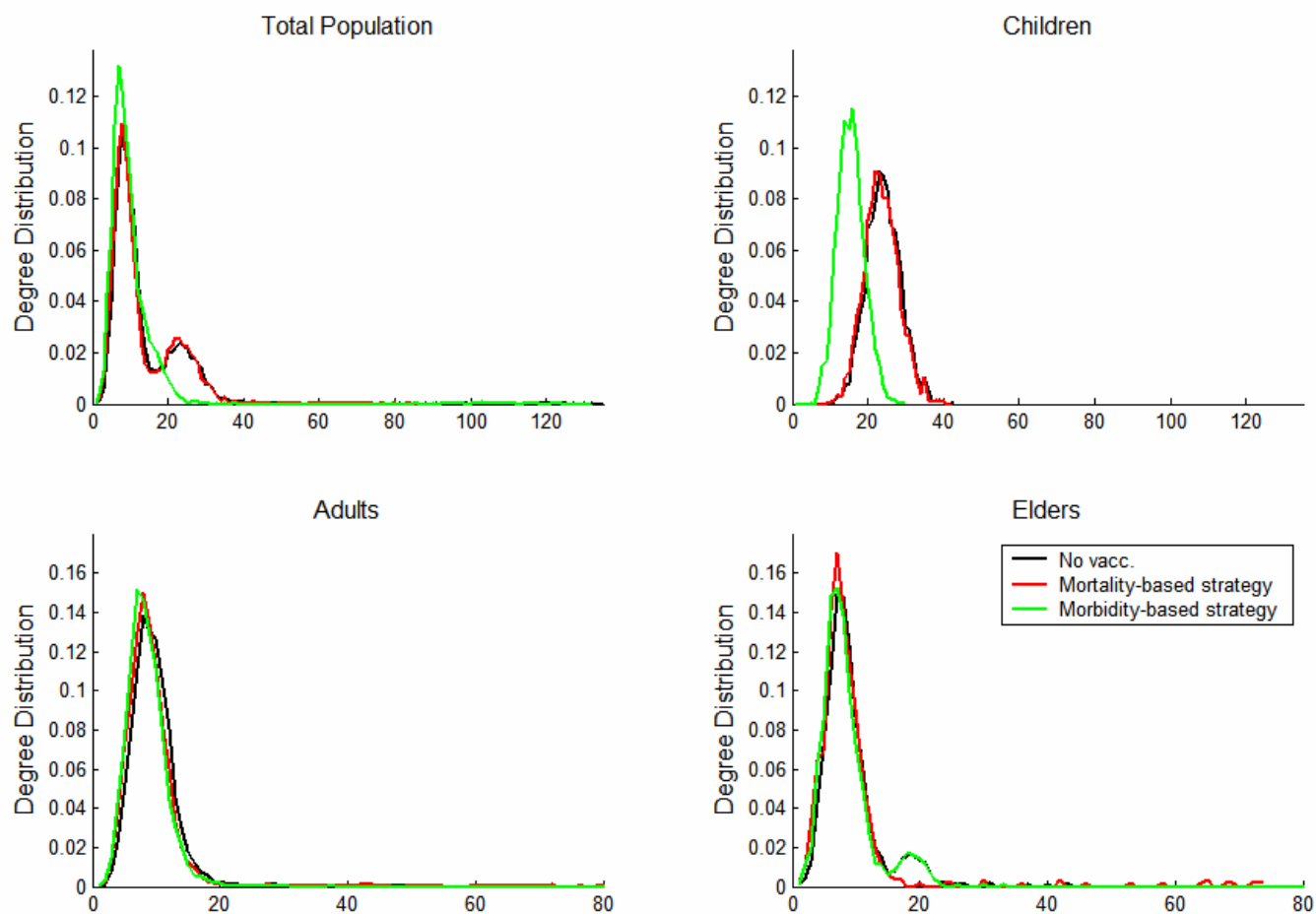


Figure S1: Degree distributions for various demographic groups before and after vaccination.

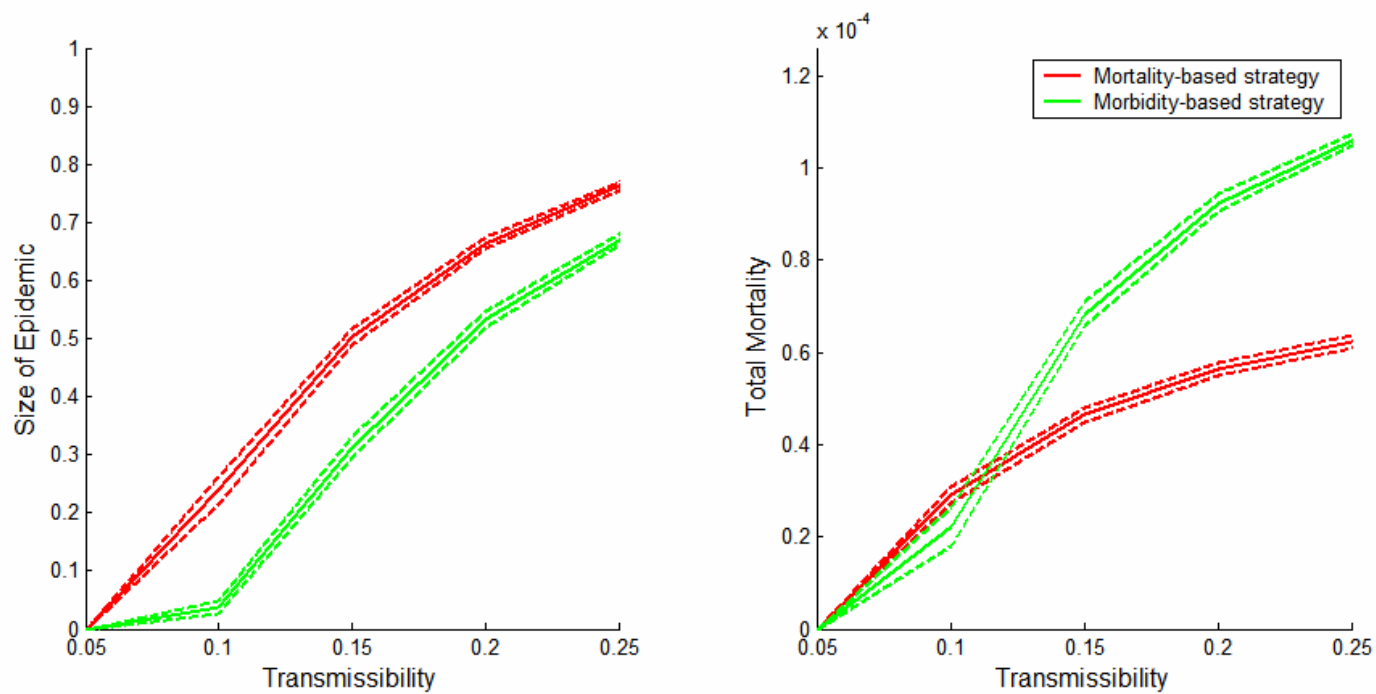


Figure S2: Variation in the size of epidemic and total mortality predicted for mortality-based (red) and morbidity-based (green) strategies across 100 networks with 15% variation in contact parameters. Dashed lines indicate standard deviations.

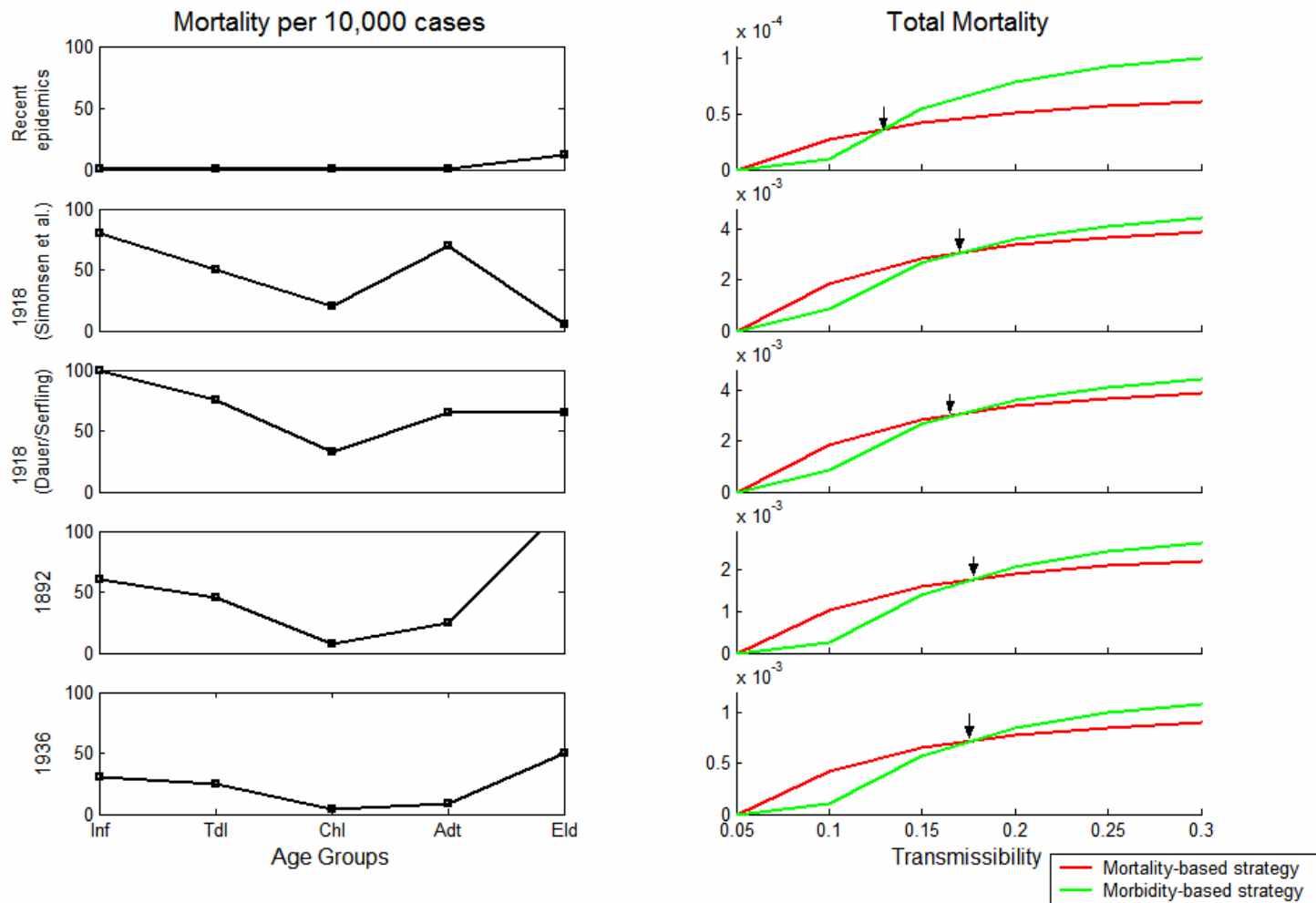


Figure S3: Epidemiological predictions for five different estimated influenza mortality distributions. Left: Mortality rates estimated for various influenza epidemics and pandemics [S8, S11, S12]. The top two distributions are considered in the main text. Right: Total mortality predicted for the mortality-based strategy (red) and morbidity-based strategy (green) assuming the corresponding distributions of mortality rates.

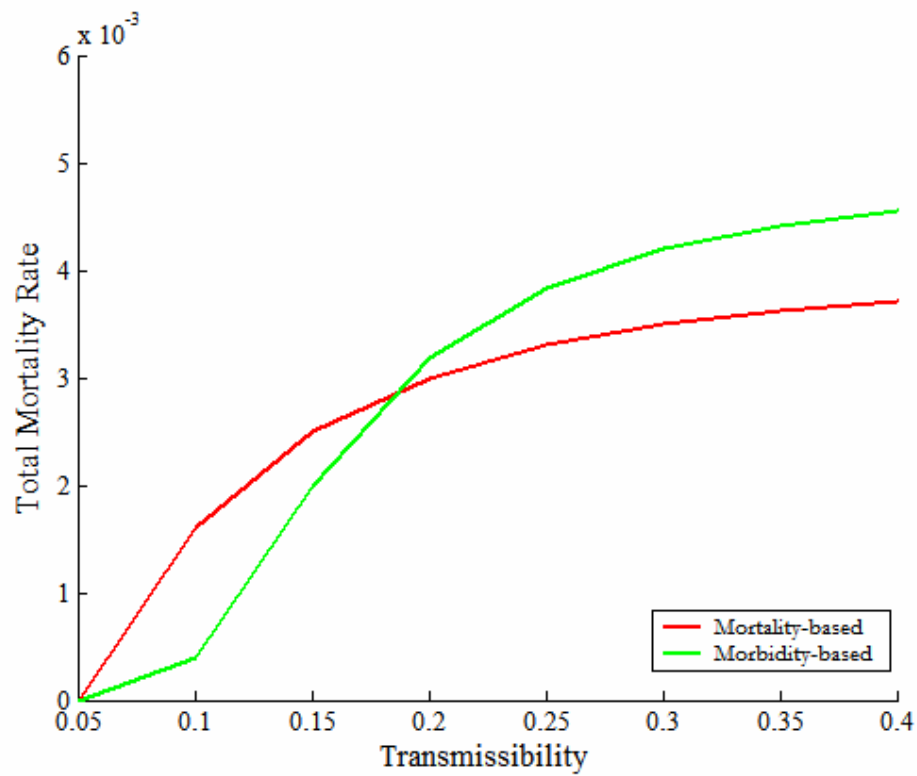


Figure S4: The total mortality at a 20% vaccination coverage level. The total mortality is lower for both strategies as compared to vaccination at a 13% coverage level (Fig 4d). However, there still exists a point after which the mortality-based strategy is superior to the morbidity-based.

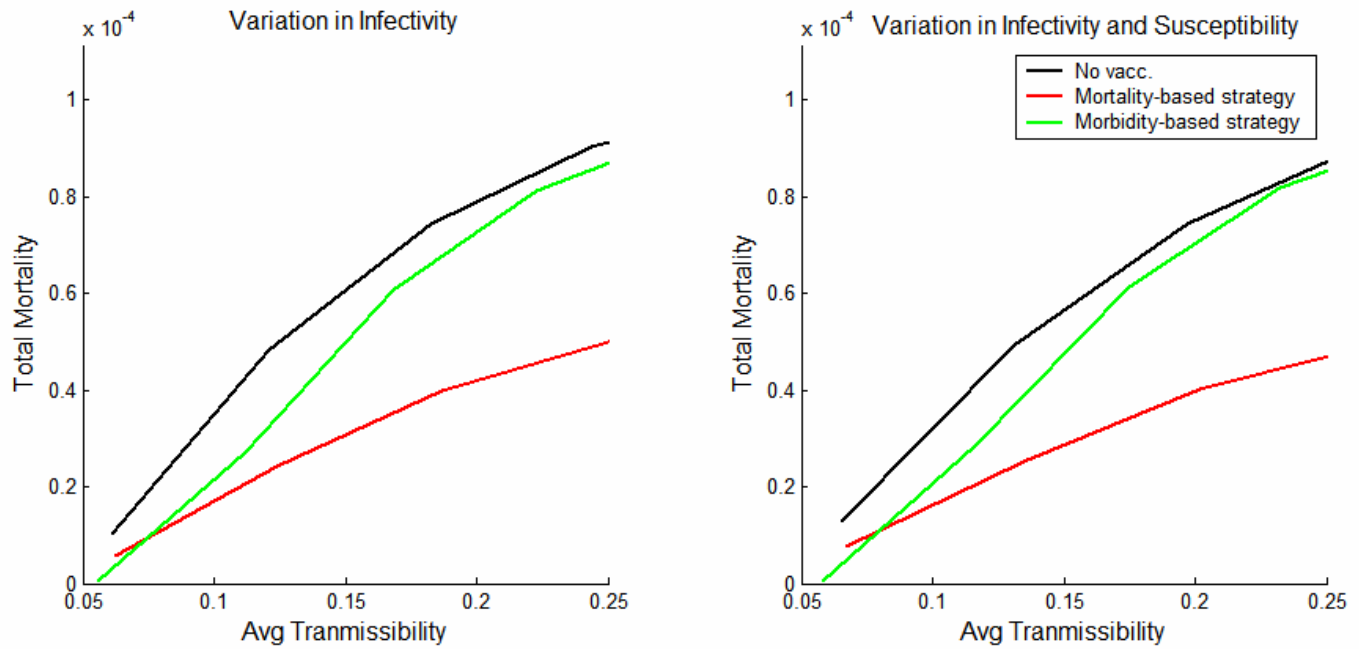


Figure S5: Simulation results for total mortality rate with variation in infectivity and/or susceptibility. The x-axis corresponds to the average transmissibility across all edges in the network.

References

- S1. Household Size, census metropolitan areas. Statistics Canada (2001)
- S2. 2001 Census Profile of British Columbia's Regions: Greater Vancouver Regional District, *BC Stats* (2003)
- S3. Vancouver School Board, December 2002 Ready Reference (2002)
- S4. The British Columbia Health Atlas, Centre for Health Services and Policy Research (2002)
- S5. Pourbohloul, B. et al. Modeling Control Strategies of Respiratory Pathogens. *Emerg. Infect Dis.* **11** (8), 1249-1256 (2005)
- S6. Meyers, L.A., Newman, M.E.J., Pourbohloul, B. Predicting epidemics on directed contact networks. *JTB (In press)*
- S7. Newman, M.E.J. Spread of epidemic disease on network. *Phys. Rev. E* **66**, 016128 (2002)
- S8. Dauer, C.C., Serfling, R.E. Mortality from Influenza, 1957-1958 and 1959-1960. *Am Rev Respir Dis* **83** (2 Suppl), 15-26 (1961)
- S9. Addy, C.L., Longini, I. M., Harber, M. A Generalized Stochastic Model for the Analysis of Infectious Disease Final Size Data. *Biometrics* **47** 961-974 (1991)
- S10. Cauchemez, S., Carrat, F., Viboud, C., Valleron, A.J., Boelle, P.Y. A Bayesian MCMC approach to study transmission of influenza: application to household longitudinal data. *Stat Med* **23** 3469-3487
- S11. Thompson, W.W. et al. Mortality associated with influenza and respiratory syncytial virus in the United States. *JAMA* **289**, 179-86 (2003)
- S12. Simonsen L. et al. Pandemic versus epidemic influenza mortality: a pattern of changing age distribution. *J. Infect. Dis.* **178**, 53-60 (1998)